·Article ·

Advances in Polar Science

doi: 10.3724/SP.J.1085.2012.00103

June 2012 Vol. 23 No. 2: 103-115

Pollen morphology of selected tundra plants from the high Arctic of Ny-Ålesund, Svalbard

YAO Yifeng[1], ZHAO Qi[2], BERA Subir[3], LI Xiaoli[4] & LI Chengsen[1*]

[1] State Key Laboratory of Systematic and Evolutionary Botany, Institute of Botany, Chinese Academy of Sciences, Beijing 100093, China;
[2] College of Life Science, Capital Normal University, Beijing 100037, China;
[3] Department of Botany, University of Calcutta, Kolkata 700019, India;
[4] Beijing Museum of Natural History, Beijing 100050, China

Received 12 April 2012; accepted 10 May 2012

Abstract Documenting morphological features of modern pollen is fundamental for the identification of fossil pollen, which will assist researchers to reconstruct the vegetation and climate of a particular geologic period. This paper presents the pollen morphology of 20 species of tundra plants from the high Arctic of Ny-Ålesund, Svalbard, using light and scanning electron microscopy. The plants used in this study belong to 12 families: Brassicaceae, Caryophyllaceae, Cyperaceae, Ericaceae, Juncaceae, Papaveraceae, Poaceae, Polygonaceae, Ranunculaceae, Rosaceae, Salicaceae, and Scrophulariaceae. Pollen grain shapes included: spheroidal, subprolate, and prolate. Variable apertural patterns ranged from 2-syncolpate, 3-colpate, 3-(-4)-colpate, 3-(-5)-colpate, 3-colporate, 5-poroid, ulcerate, ulcus to pantoporate. Exine ornamentations comprised psilate, striate-perforate, reticulate, microechinate, microechinate-perforate, scabrate, granulate, and granulate-perforate. This study provided a useful reference for comparative studies of fossil pollen and for the reconstruction of paleovegetation and paleoclimate in Svalbard region of Arctic.

Keywords **Arctic, Ny-Ålesund, pollen morphology, Svalbard, tundra plants**

Citation: Yao Y F, Zhao Q, Bera S, et al. Pollen morphology of selected tundra plants from the high Arctic of Ny-Ålesund, Svalbard. Adv Polar Sci, 2012, 23: 103-115, doi:10.3724/SP.J.1085.2012.00103

0 Introduction

Palynology is one of the most useful methods to investigate the relationship between modern pollen deposition and local vegetation across a range of ecosystems[1]. In addition, palynology allows researchers to reconstruct the past history of vegetation, climate and environment in the Quaternary[2-8]. This reconstruction of historical vegetation and climate requires surveys of modern pollen morphology as a prerequisite for identifying different fossil pollen types[9-10].

Arctic regions are sensitive to global climate change. More and more evidences (e.g., rapid melting of glacial ice, permafrost thawing) suggest that the Arctic regions are undergoing fast global warming[11-12], which will pronouncedly influence the Arctic ecosystems and biota, including plants and tundra vegetation[13-14]. Previously, a few collection of modern pollen of tundra plants from Svalbard was conducted by Rozema et al. for comparing with the fossil pollen from peat core sediments to reconstruct the past vegetation, climate and environment of that area[15]. To study the relationship between modern pollen deposition and local vegetation, and to reconstruct the past vegetation and its response to climate change on Svalbard, we collected surface soil samples and core sediments from Ny-Ålesund, Svalbard, during the Scientific Expeditions of Chinese Arctic Yellow River Station in 2008 and 2011. To prepare an index for ongoing research, we collected the polliniferous parts of living tundra plants for pollen analysis. This provided us with a baseline reference for pollen grains recovered from the surface and sub-surface core sediments. This paper presents the pollen morphology of selected tun-

* Corresponding author (email: lics@ibcas.ac.cn)

dra plants using light and scanning electron microscopy techniques, for further help in studying the relationship between modern pollen deposition and local vegetation in the Artic environment.

1 Materials and methods

1.1 Study site

The fieldwork was conducted in the high Artic of Ny-Ålesund, Svalbard (74°—81°N and 10°—35°E), which covers covers approximately 62 000 km^2 (Figure 1). The region has a mild Arctic-oceanic climate, influenced by the North Atlantic Current (a branch of the West Spitzbergen Current), which transports temperate water along the west coast of Svalbard. Due to the harsh environment on Svalbard (e.g., low temperature, short growing season (6—10 weeks), limited moisture and nutrient availability), the vegetation consists mainly of low and depressed plant types (seldom higher than 10 cm in height), including 164 vascular plant species[16].

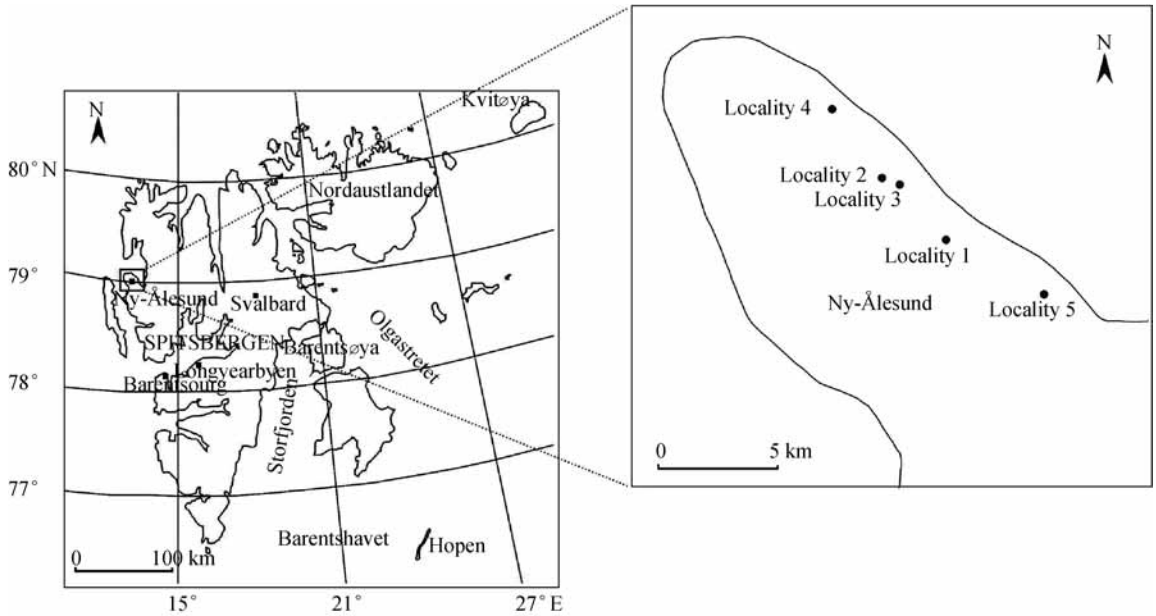

Figure 1 Map showing the sampling sites in Ny-Ålesund, Svalbard.

Ny-Ålesund (78º55'N, 11º56'E) is situated on Brøggerhalvøya, western coast of Svalbard. The annual mean air temperature and rainfall between 2001 and 2008 were -4.2℃ and 433 mm, respectively. Snow melt usually occurs in early July and snow starts to accumulate in late August[17]. The major vegetation components at Ny-Ålesund comprise polar willow (*Salix polaris*), mountain avens (*Dryas octopetala*), purple saxifrage (*Saxifraga oppositifolia*), drooping saxifrage (*S. cernua*), tufted saxifrage (*S. cespitosa*), bog saxifrage (*S. hirculus*), wood rush (*Luzula confusa*), knotweed (*Polygonum viviparum*), Arctic mouse-ear chickweed (*Cerastium arcticum*), and Arctic bell-heather (*Cassiope tetragona*).

1.2 Materials and methodology

Twenty species of tundra plants with flowers (Table 1) were collected from Ny-Ålesund during the Scientific Expeditions of Chinese Arctic Yellow River Station (eight and twelve species were collected in 2008 and 2011, respectively). Pollen grains were extracted from flower anthers and examined under Light Microscope (LM) and Scanning Electron Microscope (SEM). For LM studies, pollen grains were acetolyzed following Erdtman's method[18] and mounted in glycerine jelly. The slides were observed using a Leica DM 2500 light microscope with a 100× oil immersion lens. Measurements of pollen grains were based on 20 individual pollen grains for each species. For SEM studies, pollen grains were treated by a graded ethanol series and were dispersed on SEM stubs and sputter-coated with gold using a Hitachi E-1010 sputter coater. The samples were examined and photographed under a Hitachi S-4800 microscope at an accelerating voltage of 10 kV.

Both the polar axis diameter (P) and equatorial diameter (E) of the pollen grains were measured under LM. P/E values were calculated for each measured grain. Pollen terminologies follow Punt et al.[19] and Hesse et al.[20] . Pollen size classes are defined as: very small (<10 μm), small (10—25 μm), medium (26—50 μm), large (51—100 μm), and very large (>100 μm)[20]. In this study, shape classes in equatorial view (P/E), i.e., suboblate (0.75—0.88), spheroidal (0.88—1.14), subprolate (1.14—1.33), and prolate (1.33—2.00) are used as proposed by Punt et al.[19].

2 Results

The pollen grains were iso- or heteropolar, mainly spheroidal, subprolate and prolate, with radial or bilateral symmetry. Sizes varied from small to medium, and apertures included 2-syncolpate, 3-colpate, 3-(-4)-colpate, 3-(-5)-colpate, 3-colporate, 5-poroid, ulcerate, ulcus, and pantoporate. Psilate, striate-perforate, reticulate, microechinate, microechinate-perforate, scabrate, granulate, and granulate-perforate types of ornamentation were noted on the pollen exines. The detailed pollen characteristics of each species are shown (Table 2) and described as follows.

Table 1 Tundra plant species collected from Ny-Ålesund, Svalbard

No.	Family name	Genus name	Species name	Locality
1	Caryophyllaceae	*Silene*	*Silene wahlbergella* Chowd.	2
2			*Silene acaulis* (L.) Jacq.	1
3		*Cerastium*	*Cerastium arcticum* Lge.	1
4	Brassicaceae	*Draba*	*Draba bellii* Holm	1
5			*Draba lactea* Adams.	1
6		*Braya*	*Braya purpurascens* (R. Br.) Bunge	3
7		*Cochlearia*	*Cochlearia officinalis* L.	1
8	Polygonaceae	*Oxyria*	*Oxyria digyna* (L.) Hill	1
9		*Polygonum*	*Polygonum viviparum* L.	5
10	Scrophulariaceae	*Pedicularis*	*Pedicularis hirsuta* L.	2
11			*Pedicularis dasyantha* (Trautv.) Hadač	5
12	Ranunculaceae	*Ranunculus*	*Ranunculus pygmaeus* Wahlenb.	2
13			*Ranunculus nivalis* L.	4
14	Papaveraceae	*Papaver*	*Papaver dahlianum* Nordh.	2
15	Poaceae	*Deschampsia*	*Deschampsia alpina* (L.) Roem. & Sch.	1
16	Ericaceae	*Cassiope*	*Cassiope tetragona* (L.) D.Don	1
17	Rosaceae	*Dryas*	*Dryas octopetala* L.	1
18	Salicaceae	*Salix*	*Salix polaris* Wahlenb.	1
19	Cyperaceae	*Carex*	*Carex misandra* R.Br.	5
20	Juncaceae	*Luzula*	*Luzula confusa* (Hartm.) Lindeb.	5

Locality: 1, 78°55′01.1″N, 11°56′56″E; 2, 78°56′05.3″N, 11°49′10.3″E; 3, 78°55′49.9″N, 11°50′34.9″E; 4, 78°57′24.1″N, 11°41′16.1″E; 5, 78°54′07.4″N, 12°09′01.8″E.

Table 2 Pollen morphology of tundra plant species from Ny-Ålesund, Svalbard

Species	Pollen shape	Aperture	Polar axis /μm	Equatorial axis /μm	*P*/*E*	Exine ornamentation	Exine thickness/μm	Figure
Cerastium arcticum	spheroidal	pantoporate	(29.8-) 40.5 (-47.2)	(31.6-) 38.2 (-46.2)	1.06	microechinate-perforate	3.7	2a–2c
Silene acaulis	spheroidal	pantoporate	(21.6-) 26.8 (-31.2)	(20.2-) 25.9 (-30.6)	1.04	microechinate-perforate	2.5	2d–2f
Silene wahlbergella	spheroidal	pantoporate	(25.6-) 28.9 (-36.0)	(24.6-) 27.4 (-33.0)	1.05	microechinate-perforate	1.8	2g–2i

(To be continued on the next page)

(Continued)

Dryas octopetala	subprolate	3-colporate	(20.6-) 23.1 (-25.8)	(16.4-) 19.9 (-22.6)	1.17	striate-perforate	2.1	2j–2l
Draba lactea	subprolate	3-(-4)-colpate	(18.4-) 21.7 (-24.6)	(14.8-) 18.3 (-22.4)	1.20	reticulate	3.0	3a–3f
Draba bellii	subprolate	3-(-4)-colpate	(20.8-) 24.0 (-27.8)	(16.4-) 20.4 (-25.2)	1.18	reticulate	2.8	3g–3l, 4a–4c
Cochlearia officinalis	subprolate	3-colpate	(15.0-) 19.0 (-23.0)	(12.2-) 15.9 (-19.2)	1.20	reticulate	2.6	4d–4i
Braya pur-purascens	spheroidal	3-colpate	(27.4-) 28.4 (-30.6)	(23.6-) 25.7 (-27.0)	1.11	reticulate	3.8	4j–4l
Pedicularis dasyantha	subprolate	2-syncolpate	(15.4-) 23.4 (-27.8)	(15.0-) 18.9 (-22.2)	1.25	psilate	2.1	5a–5c
Pedicularis hirsuta	subprolate	2-syncolpate	(20.0-) 23.2 (-27.8)	(15.4-) 19.5 (-21.6)	1.20	granulate-perforate	2.0	5d–5f
Ranunculus nivalis	spheroidal	3-(-5)-colpate	(30.4-) 33.1 (-40.0)	(25.8-) 31.4 (-35.0)	1.06	microechinate-perforate	2.6	5g–5i
Ranunculus pygmaeus	spheroidal	3-(-4)-colpate	(20.2-) 24.6 (-33.8)	(21.4-) 23.3 (-27.4)	1.06	microechinate	2.8	5j–5l
Cassiope tetragona	spheroidal	3-colporate	(23.2-) 24.8 (-26.6)	(21.6-) 23.7 (-25.8)	1.05	scabrate	1.5	6a–6c
Salix polaris	spheroidal	3-colpate	(21.0-) 22.4 (-25.8)	(18.2-) 20.6 (-23.4)	1.09	reticulate-granulate	2.8	6d–6f
Papaver dahlianum	subprolate	3-colpate	(25.6-) 31.2 (-36.0)	(21.4-) 27.6 (-34.4)	1.14	microechinate-perforate	2.3	6g–6i
Oxyria digyna	spheroidal	3-colporate	(18.2-) 19.9 (-21.4)	(18.8-) 21.1 (-24.2)	0.94	verrucose-perforate	1.8	6j–6l
Polygonum viviparum	prolate	3-colporate	(40.6-) 44.7 (-47.4)	(25.6-) 31.5 (-36.4)	1.43	reticulate	3.6	7a–7c
Luzula confusa	subprolate	ulcerate	(40.0-) 48.0 (-55.6)	(34.6-) 40.1 (-46.6)	1.20	granulate	1.2	7d
Carex misandra	subprolate	5-poroid	(28.8-) 32.7 (-39.8)	(21.0-) 25.3 (-28.8)	1.31	perforate-granulate	1.3	7e
Deschampsia alpina	spheroidal	ulcus	(20.4-) 26.9 (-33.0)	(20.0-) 26.0 (-32.0)	1.03	granulate-perforate	2.0	7f

Caryophyllaceae

Cerastium arcticum Lge. (Figure 2a–2c)

Pollen grains spheroidal, 40.5 (29.8—47.2) µm × 38.2 (31.6—46.2) µm. *P*/*E* ratio 1.06. Apertures pantoporate with 18—28 pores, pore circular, approximately 4.4—4.6 µm in diameter, evenly distributed on the surface of the spheroidal grain and covered by membrane with granules. Exine ca.

3.7 µm thick. Sexine approximately three to four times as thick as the nexine. Ornamentation granulate (LM), microechinate-perforate (SEM).

Silene acaulis (L.) Jacq. (Figure 2d–2f)
Pollen grains spheroidal, 26.8 (21.6—31.2) µm × 25.9 (20.2—30.6) µm. *P/E* ratio 1.04. Apertures pantoporate with 18—24 pores, pore circular, approximately 2.8—3.3 µm in diameter, evenly distributed on the surface of the spheroidal grain and covered by a membrane with microechinates. Exine ca. 2.5 µm thick. Sexine approximately twice to three times as thick as the nexine. Ornamentation granulate (LM), microechinate-perforate (SEM). Perforation uniform in size (~ 0.7 µm).

Silene wahlbergella Chowd. (Figure 2g–2i)
Pollen grains spheroidal, 28.9 (25.6—36.0) µm × 27.4 (24.6—33.0) µm. *P/E* ratio 1.05. Apertures pantoporate with 18—20 pores, pore circular, approximately 2.1—2.5 µm in diameter, evenly distributed on the surface of the spheroidal grain and covered by a membrane with microechinates. Exine ca. 1.8 µm thick. Sexine approximately twice to three times as thick as the nexine. Ornamentation granulate (LM), microechinate-perforate (SEM). Perforation variable in size, with the maximum of 0.9 µm and the minimum of 0.1 µm.

Key to the species:

1. a. Pollen grains spheroidal. Pollen size approximately 40 µm in diameter……………………*Cerastium arcticum*
   b. Pollen grains spheroidal. Pollen size approximately 26—29 µm in diameter…………………………………2
2. a. Perforation uniform in size, approximately 0.7 µm …………………………………..*Silene acaulis*
   b. Perforation variable in size (0.1—0.9 µm) ……………………………*Silene wahlbergella*

Rosaceae

Dryas octopetala L. (Figure 2j–2l)
Pollen grains subprolate, 23.1 (20.6—25.8) µm × 19.9 (16.4—22.6) µm. *P/E* ratio 1.17. Elliptic in equatorial view and semi-triangular in polar view. Apertures 3-colporate. Colpus long, broad, sunken, margin irregular. Exine ca. 2.1 µm thick. Sexine twice as thick as nexine. Ornamentation striate (LM), striate-perforate (SEM). Muri wider than grooves, anastomosing or interweaving.

Brassicaceae

Draba lactea Adams. (Figure 3a–3f)
Pollen grains subprolate, 21.7 (18.4—24.6) µm × 18.3 (14.8—22.4) µm. *P/E* ratio 1.20. Elliptic in equatorial view and circular in polar view, sometimes 3-lobed circular. Apertures 3-(-4)-colpate. Colpus long, broader, membrane with granules. Exine ca. 3.0 µm thick. Sexine twice as thick as nexine. Ornamentation reticulate (LM and SEM). Lumina irregular in size and shape.

Draba bellii Holm (Figure 3g–3l, Figure 4a–4c)
Pollen grains subprolate, 24.0 (20.8—27.8) µm × 20.4 (16.4—25.2) µm. *P/E* ratio 1.18. Elliptic in equatorial view and circular in polar view. Apertures 3-(-4)-colpate. Colpus very long, broad, membrane with granules. Exine ca. 2.8 µm thick. Sexine thicker than nexine. Ornamentation reticulate (LM and SEM). Lumina irregular in size and shape.

Cochlearia officinalis L. (Figure 4d–4i)
Pollen grains subprolate, 19.0 (15.0—23.0) µm × 15.9 (12.2—19.2) µm. *P/E* ratio 1.20. Elliptic in equatorial view and circular in polar view. Apertures 3-colpate. Colpus very long, broad, membrane with granules. Exine ca. 2.6 µm thick. Sexine almost as thick as nexine. Ornamentation granulate-reticulate (LM), reticulate (SEM). Lumina uniform in size and shape, diameter ca. 0.6 µm.

Braya purpurascens (R. Br.) Bunge (Figure 4j–4l)
Pollen grains spheroidal, 28.4 (27.4—30.6) µm × 25.7 (23.6—27.0) µm. *P/E* ratio 1.11. Elliptic in equatorial view and circular in polar view. Apertures 3-colpate. Colpus long, rather broad, membrane with granules. Exine ca. 3.8 µm thick. Sexine thicker than nexine. Ornamentation reticulate (LM and SEM). Lumina uniform in size and shape, diameter ca. 1.15 µm.

Key to the species and groups:
1. a. Pollen grains spheroidal. P/E ratio 1.11 ....…........*Braya purpurascens*
   b. Pollen grains subprolate. P/E ratio ca. 1.20 ………………………….....................2
2. a. Lumina uniform in size and shape, diameter ca. 0.6 µm ……………………*Cochlearia officinalis*
   b. Lumina irregular in size and shape.*Draba bellii* group

Scrophulariaceae

Pedicularis dasyantha (Trautv.) Hadač (Figure 5a–5c)
Pollen grains subprolate, 23.4 (15.4—27.8) µm × 18.9 (15.0—22.2) µm. *P/E* ratio 1.25. Bilaterally symmetrical. Apertures 2-syncolpate with the ends of two colpi anastomose at the poles, colpus dividing pollen grain into equal halves. Exine ca. 2.1 µm thick. Sexine and nexine almost equal in thickness. Ornamentation psilate (LM and SEM).

Pedicularis hirsuta L. (Figure 5d–5f)
Pollen grains subprolate, 23.2 (20.0—27.8) µm × 19.5 (15.4—21.6) µm. *P/E* ratio 1.20. Bilaterally symmetrical. Apertures 2-syncolpate with the ends of two colpi anastomose at the poles, colpus dividing pollen grain into equal halves. Exine ca. 2.0 µm thick. Sexine and nexine almost equal in thickness. Ornamentation psilate (LM), granulate-perforate (SEM).

Key to the species:

a. Exine ornamentation psilate under SEM
……………………………*Pedicularis dasyantha*
b. Exine ornamentation granulate-perforate under SEM
………………………………*Pedicularis hirsuta*

Ranunculaceae

Ranunculus nivalis L. (Figure 5g–5i)
Pollen grains spheroidal, 33.1 (30.4—40.0) μm × 31.4 (25.8—35.0) μm. *P*/*E* ratio 1.06. Elliptic in equatorial view and circular in polar view. Apertures 3-(-5)-colpate. Colpus membrane with small granules. Exine ca. 2.6 μm thick. Sexine and nexine almost equal in thickness. Ornamentation granulate (LM), microechinate-perforate (SEM).

Ranunculus pygmaeus Wahlenb. (Figure 5j–5l)
Pollen grains spheroidal, 24.6 (20.2—33.8) μm × 23.3 (21.4—27.4) μm. *P*/*E* ratio 1.06. Elliptic in equatorial view and circular in polar view. Apertures 3-(-4)-colpate. Colpus membrane with small granules. Exine ca. 2.8 μm thick. Sexine thicker than nexine. Ornamentation granulate (LM), microechinate (SEM).

Key to the species:
a. Exine ornamentation microechinate under SEM
……………………………*Ranunculus pygmaeus*
b. Exine ornamentation microechinate-perforate under SEM
………………………………*Ranunculus nivalis*

Ericaceae

Cassiope tetragona (L.) D. Don (Figure 6a–6c)
Pollen grain spheroidal, 24.8 (23.2—26.6) μm × 23.7 (21.6—25.8) μm and usually four grains grouped in tetrad, arranged in tetrahedral (one grain above, three grains below; or three grains above, one below) and decussate (two grains above and two below) forms, obtuse-triangular in outline. Polar view circular in each single grain. Apertures 3-colporate. Colpus long, narrow, sunken. Exine ca. 1.5 μm thick. Sexine and nexine almost equal in thickness. Ornamentation granulate (LM), scabrate (SEM).

Salicaceae

Salix polaris Wahlenb. (Figure 6d–6f)
Pollen grains spheroidal, 22.4 (21.0—25.8) μm × 20.6 (18.2—23.4) μm. *P*/*E* ratio 1.09. Elliptic in equatorial view and circular in polar view. Apertures 3-colpate. Colpus very long, nearly reaching the poles, rather broad. Colpus membrane with fine granules. Exine ca. 2.8 μm thick. Sexine thicker than nexine. Ornamentation reticulate-granulate (LM and SEM).

Papaveraceae

Papaver dahlianum Nordh. (Figure 6g–6i)
Pollen grains subprolate, 31.2 (25.6—36.0) μm × 27.6 (21.4—34.4) μm. *P*/*E* ratio 1.14. Elliptic in equatorial view and circular in polar view. Apertures 3-colpate. Colpus very long, extending to the poles, broad, margin regular, membrane with fine granules. Exine ca. 2.3 μm thick. Sexine twice as thick as nexine. Ornamentation granulate (LM), microechinate-perforate (SEM).

Polygonaceae

Oxyria digyna (L.) Hill. (Figure 6j–6l)
Pollen grains spheroidal, 19.9 (18.2—21.4) μm × 21.1 (18.8—24.2) μm. *P*/*E* ratio 0.94. Elliptic in equatorial view and circular in polar view. Apertures 3-colporate. Colpus shallow. Exine ca.1.8 μm thick. Nexine twice as thick as sexine. Ornamentation granulate (LM), verrucose-perforate (SEM).

Polygonum viviparum L. (Figure 7a–7c)
Pollen grains prolate, 44.7 (40.6—47.4) μm × 31.5 (25.6—36.4) μm. *P*/*E* ratio 1.43. Elliptic in equatorial view and trilobate circular in polar view. Apertures 3-colporate. Colpus longer, extending to the poles. Exine at the pole areas (ca. 4.6 μm) thicker than other areas (ca. 2.7 μm). Ornamentation granulate-reticulate (LM) and reticulate (SEM).

Key to the species:
a. Pollen grains spheroidal. *P*/*E* ratio 0.94. Polar axis ca. 20 μm……………………………………..*Oxyria digyna*
b. Pollen grains prolate. *P*/*E* ratio 1.43. Polar axis ca. 44.7 μm………………………………*Polygonum viviparum*

Juncaceae

Luzula confusa (Hartm.) Lindeb. (Figure 7d)
Pollen grains subprolate or irregular, 48.0 (40.0—55.6) μm × 40.1 (34.6—46.6) μm. *P*/*E* ratio 1.20. Elliptic in equatorial view and circular in polar view. Apertures ulcerate. Exine ca. 1.2 μm thick. Sexine thicker than nexine. Ornamentation granulate (LM and SEM).

Cyperaceae

Carex misandra R. Br. (Figure 7e)
Pollen grains subprolate, 32.7 (28.8—39.8) μm × 25.3 (21.0—28.8) μm. *P*/*E* ratio 1.31. Apertures 5-poroid. One in distal pole, and four in equator. Exine ca. 1.3 μm thick. Sexine and nexine nearly equal in thickness. Ornamentation granulate (LM), perforate-granulate (SEM).

Poaceae

Deschampsia alpina (L.) Roem. & Sch. (Figure 7f)
Pollen grains spheroidal, 26.9 (20.4—33.0) μm × 26.0 (20.0—32.0) μm. *P*/*E* ratio 1.03. Circular in equatorial and polar views. Apertures ulcus, with 2.8 μm in diameter. Exine ca. 2 μm thick. Sexine about twice as thick as nexine. Or--namentation psilate (LM), granulate-perforate (SEM).

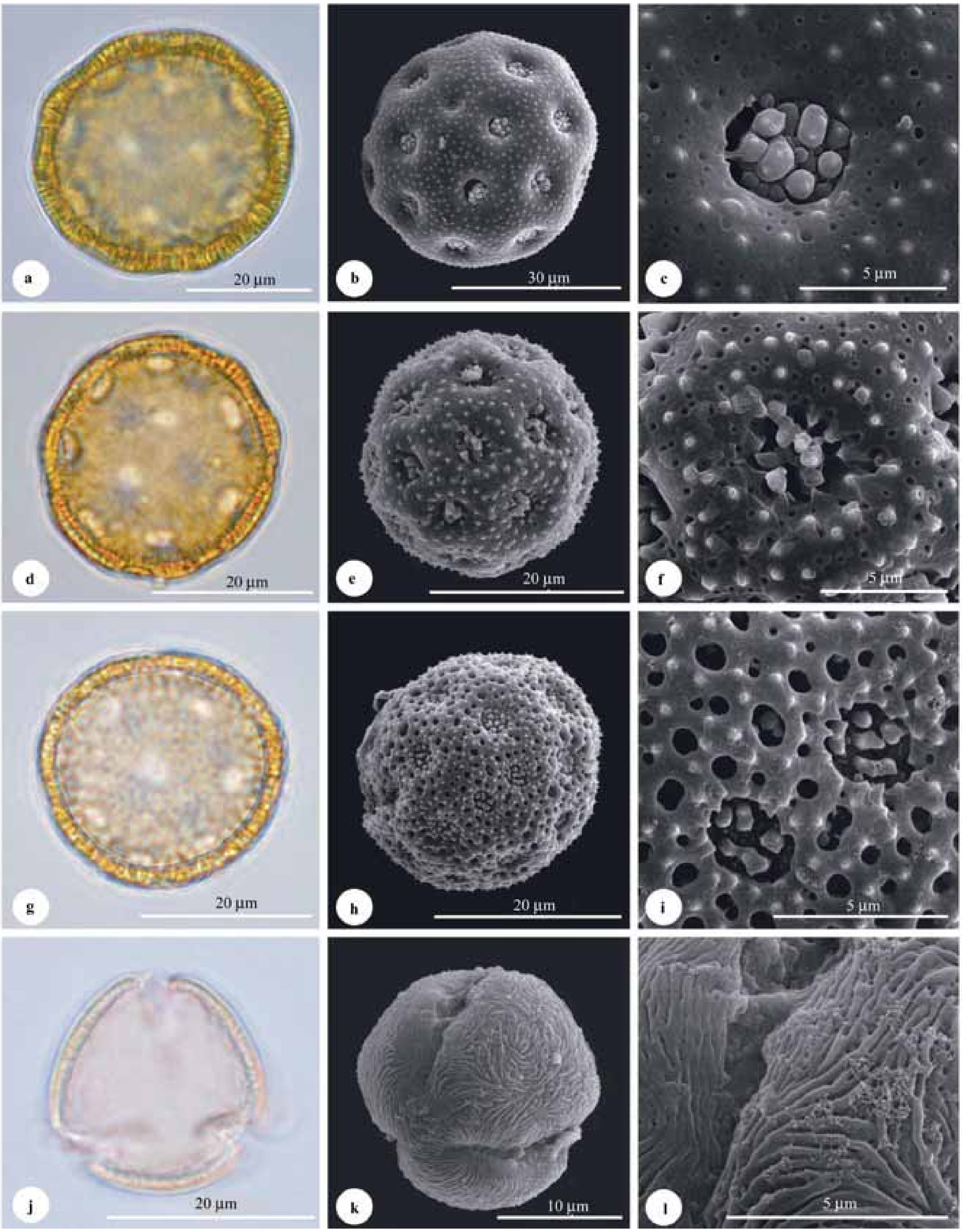

Figure 2 Pollen grains of *Cerastium arcticum* (**a**—**c**), *Silene acaulis* (**d**—**f**), *Silene wahlbergella* (**g**—**i**) and *Dryas octopetala* (**j**—**l**). **a, d, g,** Optical cross-section (LM). **b, e, h,** Outline under SEM. **c, f, i,** Aperture and exine ornamentation. **j,** Polar view (LM). **k,** Polar view (SEM). **l,** Exine ornamentation (SEM).

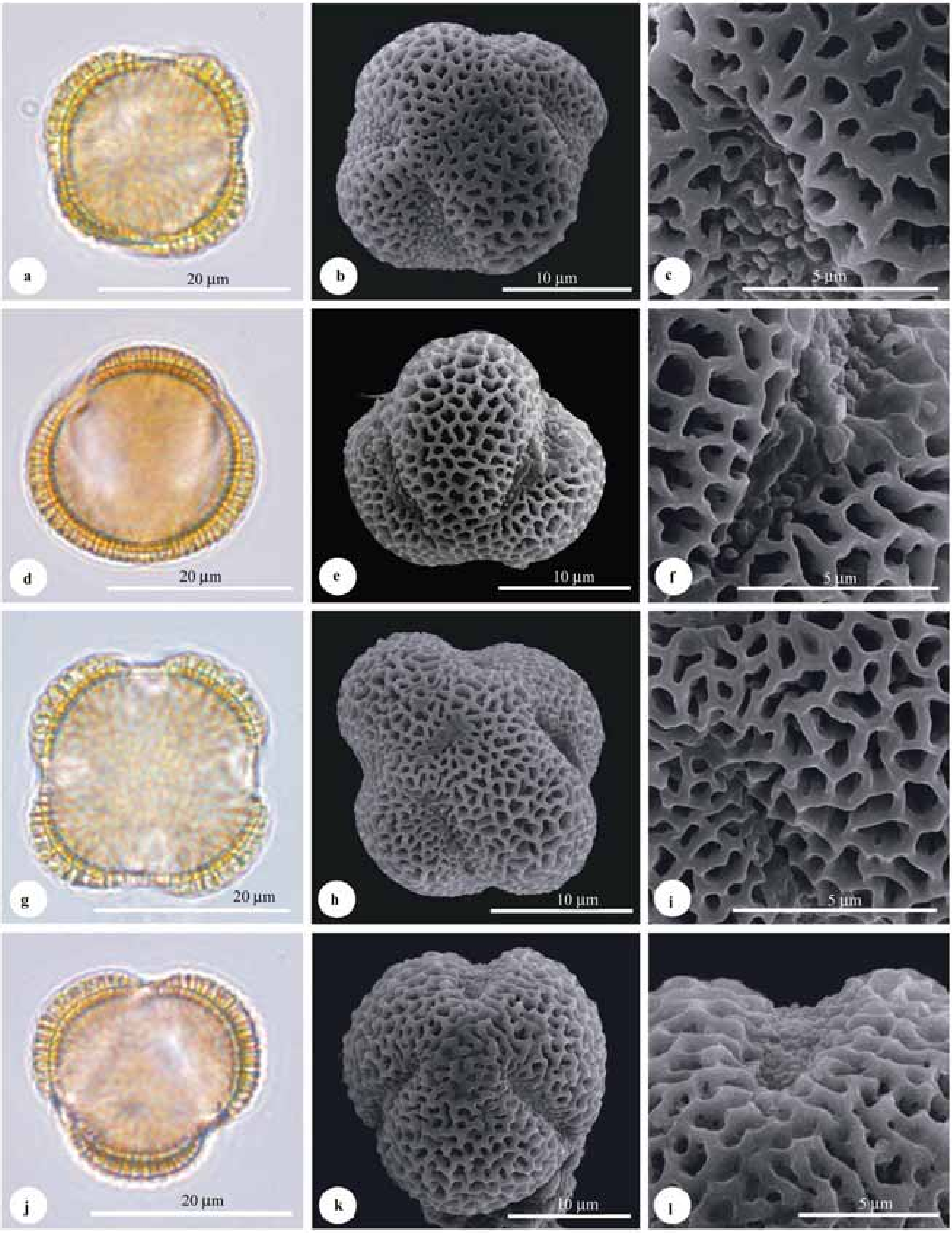

Figure 3 Pollen grains of *Draba lactea* (**a**—**f**) and *Draba bellii* (**g**—**l**). **a, d, g, j,** Polar view (LM). **b, e, h, k,** Polar view (SEM). **c, f, i, l,** Exine ornamentation (SEM).

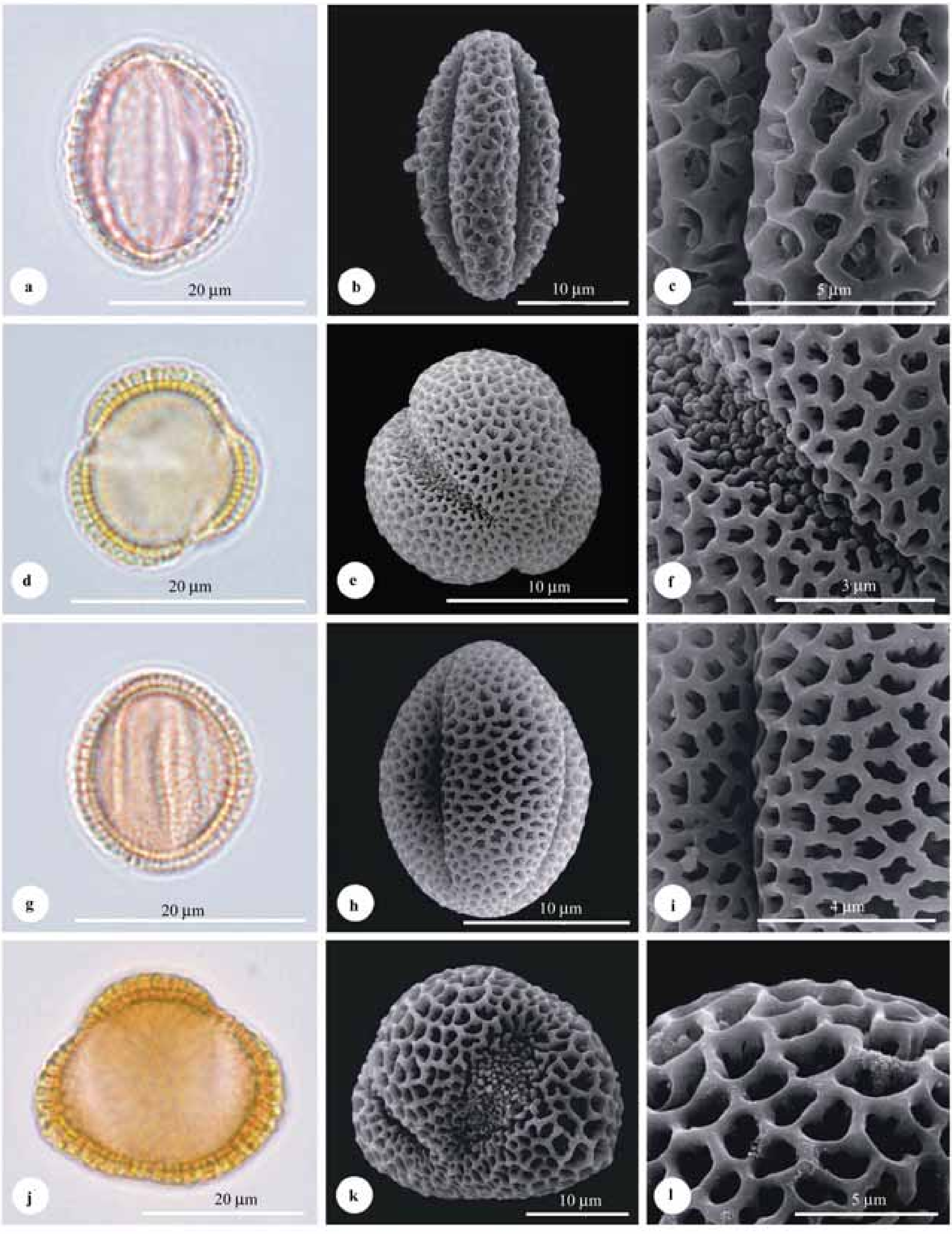

Figure 4 Pollen grains of *Draba bellii* (**a—c**), *Cochlearia officinalis* (**d—i**) and *Braya purpurascens* (**j—l**). **a, g,** Equatorial view (LM). **b, h,** Equatorial view (SEM). **c, f, i, l,** Exine ornamentation (SEM). **d, j,** Polar view (LM). **e, k,** Polar view (SEM).

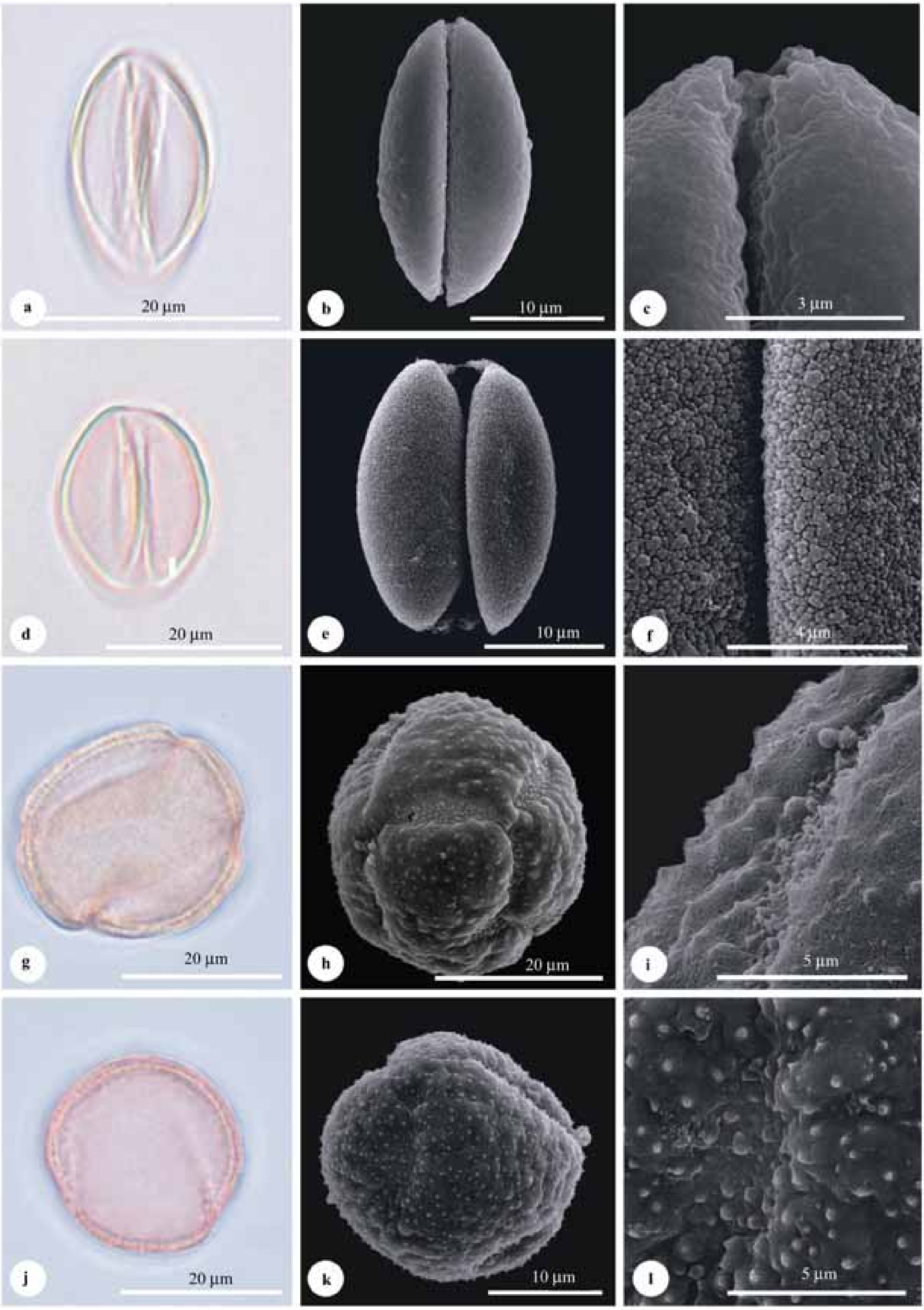

Figure 5 Pollen grains of *Pedicularis dasyantha* (**a**—**c**), *Pedicularis hirsuta* (**d**—**f**), *Ranunculus nivalis* (**g**—**i**) and *Ranunculus pygmaeus* (**j**—**l**). **a, d, j,** Equatorial view (LM). **b, e, h, k,** Equatorial view (SEM). **g,** Polar view (LM). **c, f, i, l,** Exine ornamentation (SEM).

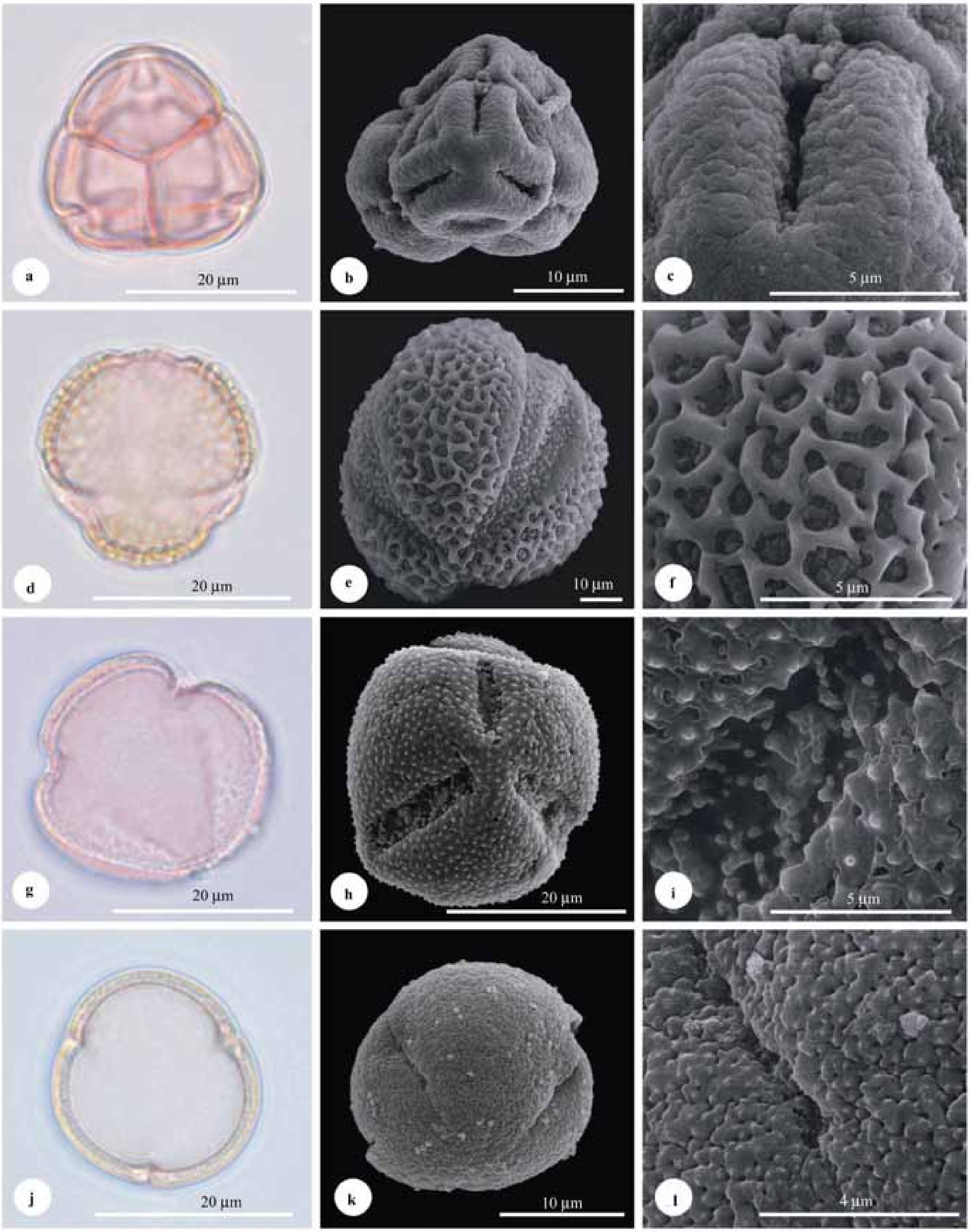

Figure 6 Pollen grains of *Cassiope tetragona* (**a**—**c**), *Salix polaris* (**d**—**f**), *Papaver dahlianum* (**g**—**i**) and *Oxyria digyna* (**j**—**l**). **a, d, g, j,** Polar view (LM). **b, h, k,** Polar view (SEM). **e,** Equatorial view (SEM). **c, f, i, l,** Exine ornamentation (SEM).

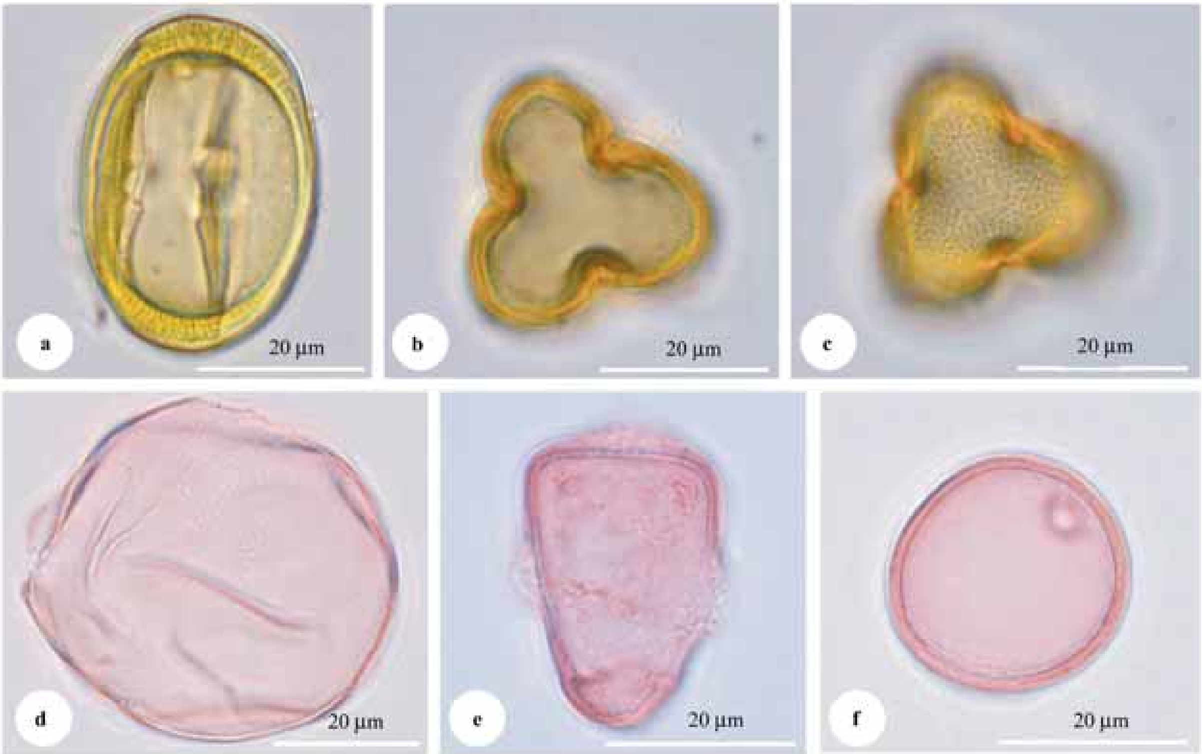

Figure 7 Pollen grains of *Polygonum viviparum* (**a**—**c**), *Luzula confusa* (**d**), *Carex misandra* (**e**) and *Deschampsia alpina* (**f**). **a, e,** Equatorial view. **b, c, d, f,** Polar view. **c,** Ornamentation in apocolpium at high focus.

3 Discussion

Pollen morphology of the 20 selected tundra plants showed considerable diversity in shape, apertural patterns and exine ornamentations. Three types of pollen shape (i.e., spheroidal, subprolate, and prolate) were recognized based on *P*/*E* ratio. Apertures included 2-syncolpate, 3-colpate, 3-(-4)-colpate, 3-(-5)-colpate, 3-colporate, 5-poroid, ulcerate, ulcus, and pantoporate. The supratectal ornamentations recorded in the pollen grains were psilate, striate-perforate, reticulate, microechinate, microechinate-perforate, scabrate, granulate, and granulate-perforate.

Previous studies have emphasized the importance of pollen morphology in plant systematics and classification[21-23]. The present study showed that the exine ornamentation patterns, presence or absence of operculum and the pollen size are important key identification factors of the plant species. The findings of this study support that the pollen morphology, especially the shape, size and exine ornamentations may help in discriminating the palynotaxa to specific level.

Many of the plants used in this study are regarded as indicators of climate change. For example, Arctic bell-heather (*Cassiope tetragona*) grows in dry localities of Svalbard, indicating warm, dry climatic conditions[16,24]. Polar willow (*Salix polaris*) has a wide distribution across Svalbard, growing in both open gravel and closed vegetation habitats, reflecting a more mild, wet habitat[16,25]. Sooty sedge (*Carex misandra*), a compact, tufted plant, is found in dry areas within dense vegetation and in gravel/rock environments. Wood rush (*Luzula confusa*) grows in loose tufts particularly in dry localities[16,24,26]. Knotweed (*Polygonum viviparum*) grows on most substrates, but grows better at favorable and nutrient-rich sites. If the palynomorphs recovered from core sediments are identified to species level, changes in climate could be reconstructed based on the ecological preferences of the mother plants. Consequently, the compilation of a pollen index of modern flora may assist in identifying the fossil palynomorphs vis-a-vis paleoclimate analysis.

Acknowledgments We would like to thank Professor Stephen Blackmore and Dr. Alexandra Wortley from Royal Botanic Garden, Edinburgh, for their valuable suggestions on this manuscript. We also thank the Chinese Arctic and Antarctic Administration (CAA), SOA for providing logistical support. This study was financially supported by the Main Direction Program of Knowledge Innovation of Chinese Academy of Sciences (Grant no. KSCX2-EW-J-1) and State Key Laboratory Systematics and Evolutionary Botany, Institute of Botany, Chinese Academy of Sciences (SKLSEB-IBCAS, Grant no. 56176G1048). Samples information and Data issued by the Resource-sharing Platform of Polar Samples (http://birds.chinare.org.cn) maintained by Polar Research Institute of China (PRIC) and Chinese National Arctic & Antarctic Data Center (CN-NADC).

References

1 Oswald W W, Brubaker L B, Hu F S, et al. Pollen-vegetation calibration

for tundra communities in the Arctic Foothills, northern Alaska. J Ecol, 2003, 91: 1022-1033.
2 Tonkov S, Panovska H, Possnert G, et al. The Holocene vegetation history of Northern Pirin Mountain, southwestern Bulgaria: Pollen analysis and radiocarbon dating of a core from Lake Ribno Banderishko. Holocene, 2002, 12(2): 201-210.
3 Xiao J L, Xu Q H, Nakamura T, et al. Holocene vegetation variation in the Daihai Lake region of north-central China: A direct indication of the Asian monsoon climatic history. Quat Sci Rev, 2004, 23: 1669-1679.
4 Tonkov S, Marinova E. Pollen and plant macrofossil analyses of radiocarbon dated mid-Holocene profiles from two subalpine lakes in the Rila Mountains, Bulgaria. Holocene, 2005, 15(5): 663-671.
5 Yi S H, Saito Y, Yang D Y. Palynological evidence for Holocene environmental change in the Changjiang (Yangtze River) Delta, China. Paleogeogr Paleoclimatol Paleoecol, 2006, 24: 103-117.
6 Zhao Y, Yu Z C, Chen F H, et al. Holocene vegetation and climate history at Hurleg Lake in the Qaidam Basin, northwest China. Rev Palaeobot Palynology, 2007, 145: 275-288.
7 Ager T A, Phillips R L. Pollen evidence for Late Pleistocene Bering Land Bridge Environments from Norton Sound, Northeastern Bering Sea, Alaska. Arct Antarct Alp Res, 2008, 40(3): 451-461.
8 Peros M C, Gajewski K. Pollen-based reconstructions of late Holocene climate from the central and western Canadian Arctic. J Paleolimn, 2009, 41: 161-175.
9 Anderson P M, Barflein P J, Brubater L B, et al. Vegetation-pollen-climate relationships for the arcto-boreal region of North America and Greenland. J Biogeogr, 1991, 18: 565-582.
10 Zhang X P, Tang L Y, Zhou Z Z, et al. A study on pollen morphology of tundra plants from Barrow, Arctic. Acta Microplaeontol Sin, 2004, 21(1): 44-52.
11 IPCC. Climate Change, The Scientific Basis, Intergovernmental Panel on Climate Change. Third Assessment Report. Impacts, Adaptation and Vulnerability. Cambridge: Cambridge University Press, 2001.
12 ACIA. Impact of a Warming Arctic: Arctic Climate Impact Assessment. Cambridge: Cambridge University Press, 2004. http://www.acia.uaf.edu.
13 Wahren C H A, Walker M D, Bret-Harte M S. Vegetation responses in Alaskan arctic tundra after 8 years of a summer warming and winter snow manipulation experiment. Glob Change Biol, 2005, 11: 537-552.
14 Alsos I G, Eidesen P B, Ehrich D, et al. Frequent long-distance plant colonization in the changing Arctic. Science, 2007, 316: 1606-1609.
15 Rozema J, Boelen P, Doorenbosch M, et al. A vegetation, climate and environment reconstruction based on palynological analyses of high arctic tundra peat cores (5 000—6 000 years BP) from Svalbard. Plant Ecol, 2006, 182: 155-173.
16 Gjaerevoll O, Rønning O I. Flowers of Svalbard. Trondheim: Tapir publishers, 1999.
17 Yoshitake S, Uchida M, Koizumi H, et al. Production of biological soil crusts in the early stage of primary succession on a High Arctic glacier foreland. New Phytol, 2010, 86: 451-460.
18 Erdtman G. Pollen Morphology and Plant Taxonomy. Angiosperms. Corrected reprint of the 1952 edition with a new addendum. New York: Hafner Publishing Company, 1966.
19 Punt W, Hoen P P, Blackmore S, et al. Glossary of pollen and spore terminology. Rev Palaeobot Palynology, 2007, 143: 1-81.
20 Hesse M, Halbritter H, Zetter R, et al. Pollen Terminology-An Illustrated Handbook. New York: Springer Wien, 2009.
21 Redondo N, Horjales M. Palynological data on the genus *Saxifraga* L. in the northeastern Iberian Peninsula. Lagascalia, 1993, 17(1): 3-19.
22 Nilsso S, Hellbom M, Smolenski W. A reappraisal of the significance of pollen in classifications of the Gentianaceae. Grana, 2002, 41: 90-106.
23 Perveen A, Qaiser M. Pollen flora of Pakistan-LXIV: Saxifragaceae. Pak J Bot, 2009, 41(4): 1531-1538.
24 Elvebakk A. Tundra diversity and ecological characteristics of Svalbard. Ecosystems of the world 3, Polar and Alpine Tundra, 1997: 347-359.
25 Van der Knaap W O. Relations between present-day pollen deposition and vegetation in Spitsbergen. Ph.D. Thesis. Laboratory of Paleabotany and Palynology, Utrecht. Groningen: Arctic centre, 1989: 15-26.
26 Rønning O I. The Flora of Svalbard. Norwegian Polar Institute, 1996.